http://www.sciencedirect.com/science/article/pii/S016943321201940X

Thermal stability of InN epilayers grown by high pressure chemical vapor deposition

Ananta R. Acharya[1], Sampath Gamage[1], M. K. Indika Senevirathna[1], Mustafa Alevli[2], Kucukgok Bahadir[3], Andrew G. Melton[3], Ian Ferguson[3], Nikolaus Dietz[1], and Brian D. Thoms[1]

[1]Department of Physics and Astronomy, Georgia State University, Atlanta, GA 30303, USA
[2] Physics Department, Marmara University, Goztepe, Istanbul, 34722, Turkey
[3] Department of Electrical and Computer Engineering, University of North Carolina at Charlotte, Charlotte, NC 28202, USA

The thermal stability of InN layers grown on sapphire by high-pressure chemical vapor deposition has been studied by thermal desorption, atomic force microscopy, x-ray diffraction, and infrared reflection measurements. Desorption products from samples grown with group V/III precursor ratios from 1200 to 4800, but otherwise identical growth conditions, have been monitored using differentially-pumped mass spectrometry while the sample temperature was ramped from room temperature to 825 °C. No significant desorption of nitrogen from the surface was observed below 630 °C, with a rapid increase of desorption of molecular nitrogen at substrate temperatures above 630 °C. No significant desorption of NH^*/NH_2^* fragments was observed. From Arrhenius plots, the activation energy for desorption of nitrogen was found to be 1.6 ± 0.2 eV. It was observed that the activation energy for the desorption of nitrogen from InN samples was independent of V/III precursor ratio. However, the temperature corresponding to the maximum desorption was found to be dependent on V/III precursor ratio, increasing from 749 °C for V/III precursor ratio of 1200 to 776 °C for V/III precursor ratio of 4800. The observed shift in the peak desorption temperature with increasing group V/III precursor ratio is attributed to the decrease in extended defects and the increase in grain size.

1. Introduction

Due to the low band gap and unique optoelectronic properties of InN, the binary cornerstone InN has attracted renewed attention in the development of group III-nitride based materials structures and device elements. The band gap energy of InN has been reported to be as low as 0.65 eV [1], which enables the utilization of the group III-nitride material system to a host of potential optoelectronic device structures such as light-emitting diodes operating from near-infrared to deep ultraviolet [2] or high efficiency photovoltaic solar cells [3]. Among the III-nitride semiconductors InN has the highest measured electron mobility, exceeding 3500 cm^2/Vs at room temperature [4]. Recent theoretical calculations using ensemble Monte Carlo method have predicted that the room temperature electron mobility of InN may be as high as 14000 cm^2/Vs [5]. This exceptional electronic transport property is most favorable for high speed electronic devices and hence InN could be an ideal material for high electron mobility transistors. In addition, InN has a potential for a wide range of applications including chemical and biological sensors [6] as well as thermoelectric devices [7] and terahertz radiation devices [8].

Despite having a number of remarkable physical properties, the utilization of InN is hampered by a limitation in the growth of high-quality InN by chemical vapor deposition (CVD) due to thermal instability and inconsistent surface morphologies. One of the ways to avoid thermal dissociation is to grow InN epilayers at low temperature. But at low temperature the cracking

Published at: Applied Surface Science **268** pp.1-5 (2013); Available online 8 November 2012

efficiency of ammonia precursor is extremely low, requiring a large group V/III precursor ratio for low-pressure CVD growth [9]. It has been reported that InN and related alloys can be grown at much higher temperatures through surface stabilization at higher reactor pressures [9]. High-pressure chemical vapor deposition (HPCVD) has been shown to be a viable approach to produce high quality III-N epilayers [9].

In recent decades several research groups explored the epitaxial growth of InN layers using techniques such as plasma-assisted molecular beam epitaxy (PA-MBE), low- and high-pressure metal organic chemical vapor deposition (MOCVD), and hydride vapor phase epitaxy (HVPE). Fewer studies have been done on the thermal stability and decomposition behavior of the InN epilayers [10-14] than have been reported for electronic, structural and optical properties. Thermal stability is very important factor in the growth process as well for the device performance and life time. However, these studies have shown inconsistent results for the decomposition activation energy ranging from 1.15 eV to 3.4 eV. Huang *et al*. [10] studied the thermal stability of MOCVD-grown InN in a nitrogen environment using in-situ laser reflectance. The reported activation energy and onset temperature of nitrogen desorption were 2.1 ± 0.1 eV and 500 °C respectively. Togashi *et al.* [11] studied the temperature dependent decomposition of HVPE grown N-polar InN in a nitrogen ambient. The estimated values of the activation energy and onset temperature of nitrogen desorption were 3.33 eV and 610 °C respectively. In another study [12] the same authors observed a polarity dependent activation energy when the samples were annealed in hydrogen ambient. In that work N-polar InN displayed an activation energy of 1.10 eV and desorption onset temperature was 350 °C while In-polar InN showed an activation energy of 1.74 eV. These results indicate that the decomposition of InN is enhanced by the presence of hydrogen and the activation energy is dependent on growth direction. Ambacher *et al.* [13] performed experiments on the decomposition of low pressure chemical vapor deposition (LPCVD)-grown InN. The sample was put in a quartz tube evacuated to less than 1.5×10^{-8} Torr and the desorbed species were measured with a QMS. Desorption spectra were measured by heating samples inside the quartz tube with a linear temperature ramp (20 °C/min) from room temperature to 1100 °C. From the Arrhenius plot, the calculated activation energy was 3.48 eV and the observed onset of nitrogen desorption temperature was 630 °C. Koblmüller *et al.* [14] studied the thermal instability of InN (0001) grown by PA-MBE, monitoring the indium desorption under vacuum conditions using QMS. From their analysis, different values of the activation energy were found for two temperature regimes, lower temperature (560 – 595 °C) and higher temperature (605 – 645 °C). In higher temperature regime, the reported value of the activation energy was 1.15 eV whereas in lower temperature regime, the activation energy was measured to be 4.4 eV and the onset of temperature for InN decomposition was 560 °C. The reported variation in the activation energy of InN epilayers indicates a strong influence of the growth process on the thermal stability and physical properties of InN, motivating our studies on the thermal stability of InN samples grown under HPCVD conditions. In this paper, we report the results of an investigation of the thermal stability of HPCVD-grown InN epilayers by temperature programmed desorption including a determination of the activation energy for molecular nitrogen evolution.

2. Experimental

The indium nitride (InN) epilayers studied in this work were grown on sapphire substrates at a temperature of 832 °C and a reactor pressure of 15 bar. Ammonia (NH_3) and trimethylindium

(TMI) were used as group-V and group-III precursors, respectively. The precursors were embedded into a nitrogen carrier gas stream. In order to avoid gas phase reactions during the growth process they were injected separately by pulsed injection which was temporally controlled, maintaining a constant reactor pressure at all times. The carrier gas flow was adjusted so that the gas flow velocity above the sample surface was kept constant. Details of the HPCVD reactor system, the growth configuration, as well as real-time optical characterization techniques employed have been published elsewhere [15, 16]. The four InN samples discussed in this work were grown under identical process conditions, varying only the group V/III precursor ratio from 1200 to 4800.

Infrared (IR) reflection measurements were performed at room temperature over the frequency range of 450–7000 cm^{-1} using a fast Fourier transform infrared spectrometer and mercury cadmium telluride detector [17]. All IR reflection spectra were taken under near normal (~8°) incident light arrangement to minimize the anisotropy effect in InN films. The surface morphology of the layers was analyzed by atomic force microscopy (AFM). The crystalline structure of the InN layers was characterized with ω - 2θ x-ray diffraction (XRD) measurements which confirmed the crystallite orientation of (01-11) for these polycrystalline films as observed in the author's earlier work [18].

The InN samples were rinsed with isopropyl alcohol before transfer into the ultra high vacuum (UHV) chamber. The samples were mounted on a tantalum sample holder and held in place by tantalum clips. The details of the UHV system and sample mount have been reported elsewhere [19]. The base pressure of our UHV system was 1.7×10^{-10} Torr. To remove the surface contaminants due to the exposure to the air, sample cleaning was performed by sputtering with 1 keV nitrogen ions followed by atomic hydrogen cleaning. The details of sputtering and atomic hydrogen cleaning are also published elsewhere [18, 20]. Auger electron spectroscopy (AES) was used to monitor the cleanliness of the samples. AES was also used to determine the composition of the near surface region which showed equal amounts of indium and nitrogen indicating no In adlayers or droplets after surface preparation in UHV.

The desorption study was carried out by heating the samples from room temperature to 825 °C by ramping at the rate of 30 °C per minute using a temperature controller. The samples were heated by the bombardment of electrons from the back of the tantalum sample holder and the temperatures were measured using a chromel-alumel thermocouple attached on the mount next to the sample. In order to check the reliability of the temperature measurements by thermocouple, an optical pyrometer was also used. No significant difference in temperatures was observed between the two measurements. Desorption products were measured with a differentially-pumped quadrupole mass spectrometer (QMS) having a pinhole in the nose cone. The sample was placed approximately 5 mm from the nose cone of the mass spectrometer and the desorbed species were monitored with the QMS while the sample temperature was ramped.

3. Results and discussion

The desorption of molecular nitrogen from InN with the increase of temperature is shown in Fig. 1. No significant NH_3 (17 amu) desorption was observed. The 14 and 28 amu desorption signals showed identical behavior at T > 600 °C. This confirms desorption of nitrogen from the InN samples in the form of N_2. However, below 600 °C, a small desorption peak of 28 amu was observed with no desorption of 14 amu. The 28 amu signal desorbed below 600 °C is attributed to carbon monoxide. In all four samples, desorption of nitrogen started at around 630 °C, increased

rapidly with increasing temperature, and peaked before decreasing as shown in Fig. 2. After attaining the peak value, the desorption rate decreased with the increase of temperature indicating that the film was getting thinner until the entire film was desorbed completely. Though the signal to noise ratio for indium desorption was not as good as that for nitrogen, the desorption of indium was observed similar to that of nitrogen (not shown). In all InN samples studied, the shape of desorption curves was similar. However, the temperature corresponding to the maximum desorption was found to be different as seen in Fig. 2.

The experimental IR reflection spectra were analyzed using a multilayer stack model [21] and a Lorentz-Drude model for the dielectric of the medium to obtain the thickness of the layers. From the analysis, the film thicknesses of 270 nm, 360 nm, 320 nm and 270 nm were obtained for the samples grown with group V/III precursor ratios of 1200, 2400, 3600 and 4800 respectively. Ideally, a direct correlation of the film thicknesses with the area under the desorption curves (Fig.2) is expected. However, if the films contain different amount of voids and defects, the thicknesses of the films would not correlate with the area under the desorption curves. Using the effective medium theory, the void fraction was calculated in each sample. The void fractions were 0.023, 0.23, 0.09 and 0.26 for the samples grown with group V/III precursor ratios of 1200, 2400, 3600 and 4800 respectively. Corrected values for the total thickness accounting for the void fraction were calculated and these values correlate very well with the area under the desorption curves.

Fig. 3 shows 1μm × 1μm AFM images obtained from three of the four InN samples grown with group V/III molar precursor ratios of 1200, 2400, and 4800. The results show average grain sizes of 176 nm, 200 nm and 224 nm for the three films, respectively, indicating that average grain size increases with the increasing group V/III precursor ratio. The increase in the average grain area with increasing V/III molar precursor ratio suggests a decrease in extended defects for higher V/III molar precursor ratios [22]. It has been reported that thermal stability decreases with the decrease of grain size [23]. That is, as the extended defects are reduced and grain size is increased, the material is more thermally stable and a longer or higher temperature annealing is required to desorb InN films. This is consistent with the result reported here that films grown with higher group V/III ratios also exhibit larger grain sizes and yield a higher temperature of maximum desorption.

Desorption curves were used to calculate an activation energy for the desorption of nitrogen from each sample was by an Arrhenius analysis. The desorption rate, R, is assumed to be described by the equation [24],

$$R = - d\theta/dt = \theta^n \nu_n e^{-(E_a/kT)} \quad (1)$$

where θ is the surface coverage, n is the order of desorption, ν is the pre exponential factor, E_a is the activation energy, k is the Boltzmann constant and T is the temperature in Kelvin. The desorption order was assumed to be zero since decomposition leaves the surface in an identical configuration. So the desorption rate would then be given by

$$R = - d\theta/dt = \nu_0 e^{-(E_a/kT)} \quad (2)$$

For each of the four samples studied here the natural log of the desorption rate was plotted versus inverse temperature to determine the activation energy for the desorption of nitrogen from InN. In

each case, only the leading edge of the desorption curve (Fig. 2) was used to find the activation energy. Fig. 4 shows the fitting used to determine the activation energy for one of the samples in this work. The value of the activation energy was found to be 1.6 ± 0.2 eV for all four samples showing that the activation energy of InN layers is independent of group V/III precursor ratio. The activation energies for thermal decomposition of InN reported previously together with our results are summarized in Table 1.

In this work, the decomposition of InN was studied under high vacuum conditions. The desorbed species were measured with a QMS, keeping the nose cone of the mass spectrometer in close proximity (~5 mm) to front of the sample. The onset of the InN decomposition was observed around 630 °C. From the Arrhenius plots of each sample the calculated value of activation energy was found out to be 1.6 ± 0.2 eV. Although the activation energy as determined in previous studies varies by a large amount, the value determined in this work is close to that reported by Koblmüller *et al.* [14] for the high temperature regime and also similar to the value given by Huang *et al*. [10]. These decomposition studies show that InN has also a large range for the activation energy (1.15 – 3.4 eV) similar to the range reported for decomposition of GaN (0.34 – 3.62 eV) [25, 26]. For GaN, the decomposition rate is reported to depend upon growth reactor designs and flow dynamics [26].

The studies on thermal stability of InN also indicate that a number of factors may affect the decomposition rate and activation energy. The analysis results summarized in Table 1 were performed on InN layers grown by five different methods which resulted in at least three different growth directions. Although there are wide variations in the activation energy reported, no clear trend with growth technique or film orientation is apparent. However, from the data in Table 1 it is clear that the onset temperatures are similar (500-630 °C) for measurements made in nitrogen or vacuum ambient while considerably lower in the presence of hydrogen (<350 °C). The activation energy measured in a hydrogen background is also at the low end of the range compared with measurements made when no hydrogen is introduced. Hydrogen in the InN layers may react or be evolved during the decomposition process. Hydrogen may also be liberated from metals during the heating of the samples. The effects of unintentional hydrogen introduction are difficult to account for or to eliminate. We suggest that the effects of hydrogen on the decomposition may add to the wide variation in measured activation energies reported.

4. Conclusion

In summary, the thermal stability of HPCVD-grown InN epilayers has been studied by thermal desorption and infrared measurements. The desorption of nitrogen from the InN surface started around 630 °C with a calculated activation energy of 1.6 ± 0.2 eV, which is independent from the group V/III precursor ratio. The temperature at which the maximum desorption was observed shifted with increasing group V/III precursor ratio from 749 °C for a ratio 1200 to 776 °C for a ratio 4800. The analysis of surface topography suggests that this shift is related to the decreased extended defects and increased grain size with increasing group V/III precursor ratio.

Acknowledgement

This work is financially supported by AFOSR under award # FA9550-10-1-0097 and GSU-RPE.

References

[1] K. M. Yu, Z. Liliental-Weber, W. Walukiewicz, W. Shan, J. W. Ager, S. X. Li, R. E. Jones, E. E. Haller, Hai Lu, and William J. Schaff, Appl. Phys. Lett. 86 (2005) 071910.

[2] M. Higasshiwaki and T. Matsui, Jpn. J. Appl. Phys. 41 (2002) L540.

[3] J. Wu, W. Walukiewicz, K. M. Yu, W. Shan, J. W. Ager, E. E. Haller, Hai Lu, William J. Schaff, W. K. Metzger, and Sarah Kurtz, J. Appl. Phys. 94 (2003) 6477.

[4] T. B. Fehlberg et al., Jpn. J. Appl. Phys. 45 (2006) L1090.

[5] V. M. Polyakov and F. Schweirz, Appl. Phys. Lett. 88 (2006) 032101.

[6] H. Lu, W.J. Schaff, L.F. Eastman, J. Appl. Phys. 96 (2004) 3577.

[7] S. Yamaguchi, R. Izaki, N. Kaiwa, S. Sugimura, A. Yamamoto, Appl. Phys. Lett. 84 (2004) 5344.

[8] Y. M. Meziani, B. Maleyre, M. L. Sadowski, S. Ruffenach, O. Briot, W. Knap, Phys. Stat. Sol. (a) 202 (2005) 590.

[9] N. Dietz, M. Strassburg, and V. Woods, J. Vac. Sci. Technol. A 23 (2005) 1221.

[10] Y.Huang, H. Wang, Q.Sun, J.Chen, J.F. Wang, Y.T. Wang, and H.Yang, J. Crystal Growth 281 (2005) 310.

[11] R. Togashi, T. Kamoshita, Y. Nishizawa, H. Murakami, Y. Kumagai, and A. Koukitu, Phys. Stat. Sol. (c) 5 (2008) 1518.

[12] R. Togashi, T. Kamoshita, H.Adachi, H. Murakami, Y. Kumagai, and A. Koukitu, Phys. Stat. Sol.(c) 6 (2009) S372.

[13] O. Ambacher, M.S. Brandt, R. Dimitrov, T. Metzger, M. Stutzmann, R. A. Fischer, A. Miehr, A. Bergmaier, and G. Dollinger, J. Vac. Sci. Technol. B 14 (1996) 3532.

[14] G. Koblmüller, C. S. Gallinat, and J. S. Speck, J. Appl. Phys. 101 (2007) 083516.

[15] N. Dietz, M. Alevli, V. Woods, M. Strassburg, H. Kang, I. T. Ferguson, Phys. Stat. Sol. (b) 242 (2005) 2985.

[16] V. Woods, N. Dietz, Mat. Sci. Eng. B 127 (2006) 239.

[17] Z. G. Hu, M. Strassburg, A. Weerasekara, N. Dietz, A. G. U. Perera, M. H. Kane, A. Asghar, and I. T. Ferguson, Appl. Phys. Lett. 88 (2006) 061914.

[18] A. R. Acharya, M. Buegler, R. Atalay, N. Dietz, B. D. Thoms, J.S. Tweedie, and R. Collazo, J. Vac. Sci. Technol. A 29 (2011) 041402.

[19] V. J. Bellitto, B. D. Thoms, D. D. Koleske, A. E. Wickenden, and R. L. Henry, Surf. Sci. 430 (1999) 80.

[20] R. P. Bhatta, B. D. Thoms, M. Alevli, and N. Dietz, Surf. Sci. 601 (2007) L120.

[21] A. B. Weerasekara, Z. G. Hu, N. Dietz, A. G. U. Perera, A. Asghar, M. H. Kane, M. Strassburg, and I. T. Ferguson, J. Vac. Sci. Technol. B 26 (2008) 52.

[22] G. Durkaya, M. Buegler, R. Atalay, I. Senevirathna, M. Alevli, O. Hitzemann, M. Kaiser, R. Kirste, A. Hoffmann, and N. Dietz, Phys. Stat. Sol.(a) 207, 1379 (2010) 1379.

[23] Ghenadii Korotcenkov, and Beognki Cho, "Second International Conference on Computer Research and Development", IEEE (2010) 461.

[24] P. A. Redhead, Vacuum 12 (1962) 203.

[25] D. D. Koleske, A. E. Wickenden, R. L. Henry, M. E. Twigg, J. C. Culbertson, R. J. Gorman, Appl. Phys. Lett. 73 (1998) 2018.

[26] D. D. Koleske, A. E. Wickenden, R. L. Henry, J. C. Culbertson, M. E. Twigg, J. Cryst.Growth 223 (2001) 466.

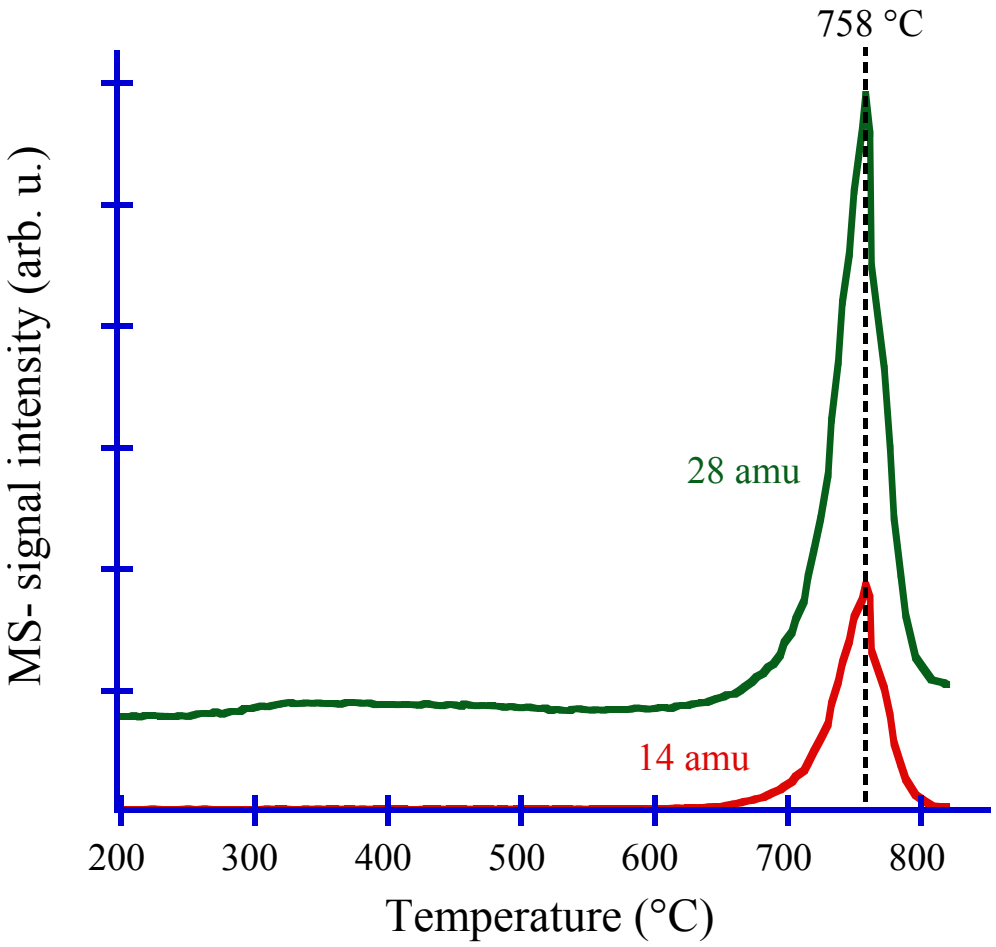

Fig. 1. Mass spectrometer signal intensity of nitrogen species desorbed from InN as a function of temperature. These data were collected from InN layer grown with a V/III precursor ratio of 2400 although data from other samples are similar.

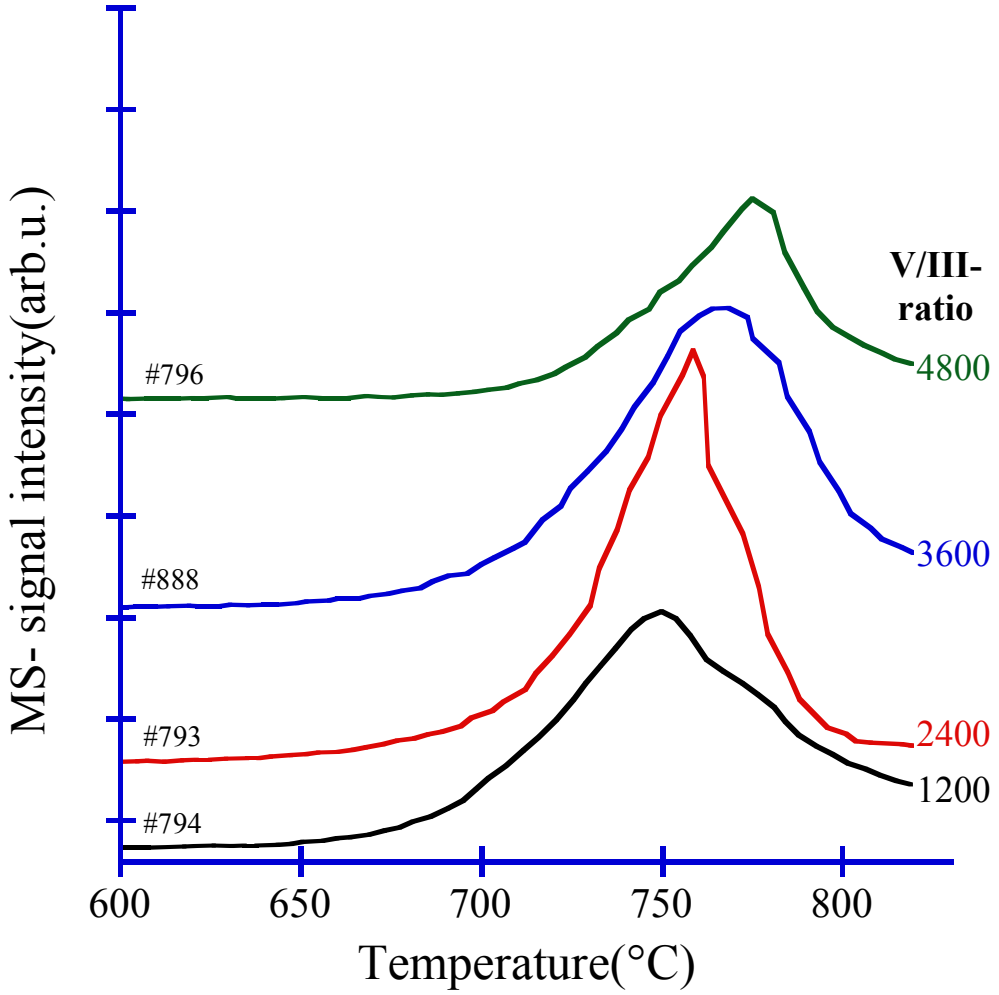

Fig. 2. Mass spectrometer signal intensity for 28 amu as a function of temperature measured while sample temperature was increased linearly at 30 °C /min from InN samples of V/III precursor ratios varying from 1200 to 4800. Inset shows the linear dependence of temperature corresponding to the maximum desorption on group V/III precursor ratio.

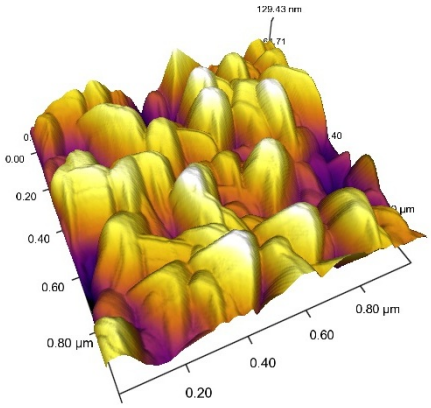

(a)

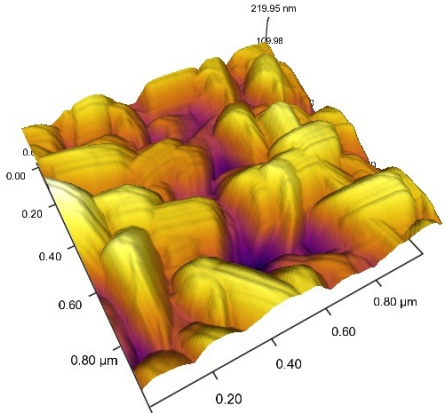

(b)

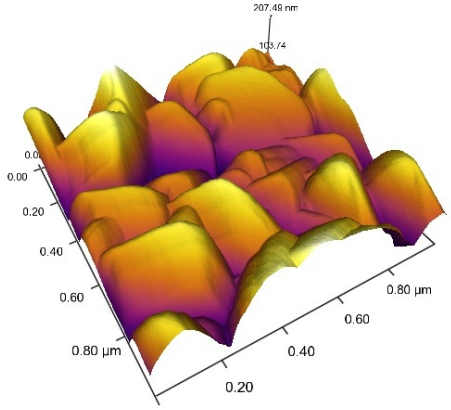

(c)

Fig. 3. 1µm × 1µm AFM images for InN epilayers deposited on sapphire (0001) substrates. The layers were grown with group V/III molar precursor ratios of (a) 1200 (b) 2400, and (c) 4800.

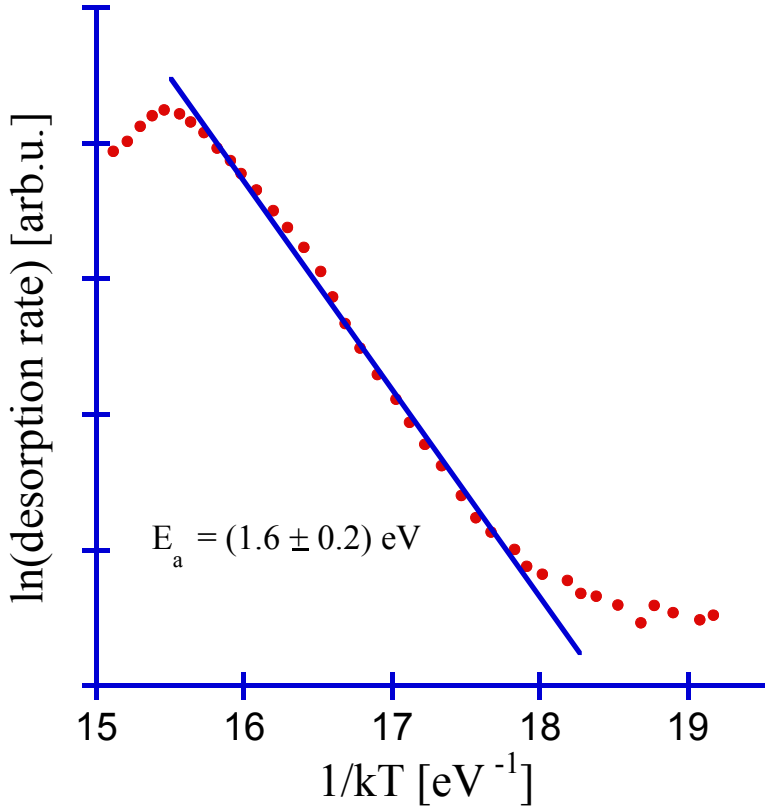

Fig. 4. Natural log of 28 amu mass spectrometer signal as a function of 1/kT for InN sample with V/III-ratio of 2400 while sample temperature was linearly increased at 30 °C /min. The activation energy was calculated using the slope of the best fit line.

Table 1. Summary of the results for thermal stability of InN reported in the literature and current work.

Authors (Reference)	Growth technique	Growth direction	Measurement technique	Annealing medium	Desorption onset temp. ($^{\circ}$C)	Activation energy (eV)
Huang *et al*. (Ref. 10)	MOCVD	-	Laser reflection	N_2	500	2.1 ± 0.1
Togashi *et al*. (Ref. 11)	HVPE	$[000\bar{1}]$	-	N_2	610	3.33
Togashi *et al*. (Ref. 12)	HVPE	[0001]	-	N_2	550	-
Togashi *et al*. (Ref. 12)	HVPE	$[000\bar{1}]$	-	H_2	< 350	1.10
Togashi *et al*. (Ref. 12)	HVPE	[0001]	-	H_2	< 350	1.74
Ambacher *et al.* (Ref. 13)	LPCVD	-	QMS	Vacuum	630	3.48
Koblmüller *et al.* (Ref. 14)	PA-MBE	$[000\bar{1}]$	QMS	Vacuum	560	1.15 (high temp. regime)
Koblmüller *et al.* (Ref.14)	PA-MBE	$[000\bar{1}]$	QMS	Vacuum	560	4.4 (low temp. regime)
Current work	HPCVD	$[01\bar{1}1]$	QMS	Vacuum	630	1.6 ± 0.2